Molecules and Cells

DDX53 Promotes Cancer Stem Cell-Like Properties and Autophagy

Hyuna Kim[1,2], Youngmi Kim[1,2], and Dooil Jeoung[1,*]

[1]Department of Biochemistry, Kangwon National University, Chunchon 24341, Korea, [2]These authors are contributed equally to this work.
*Correspondence: jeoungd@kangwon.ac.kr
http://dx.doi.org/10.14348/molcells.2017.2258
www.molcells.org

Although cancer/testis antigen DDX53 confers anti-cancer drug-resistance, the effect of DDX53 on cancer stem cell-like properties and autophagy remains unknown. MDA-MB-231 ($CD133^+$) cells showed higher expression of DDX53, SOX-2, NANOG and MDR1 than MDA-MB-231 ($CD133^-$). DDX53 increased *in vitro* self-renewal activity of MCF-7 while decreasing expression of DDX53 by siRNA lowered *in vitro* self-renewal activity of MDA-MB-231. DDX53 showed an interaction with EGFR and binding to the promoter sequences of EGFR. DDX53 induced resistance to anti-cancer drugs in MCF-7 cells while decreased expression of DDX53 by siRNA increased the sensitivity of MDA-MB-231 to anti-cancer drugs. Negative regulators of DDX53, such as miR-200b and miR-217, increased the sensitivity of MDA-MB-231 to anti-cancer drugs. MDA-MB-231 showed higher expression of autophagy marker proteins such as ATG-5, $pBeclin1^{Ser15}$ and LC-3I/II compared with MCF-7. DDX53 regulated the expression of marker proteins of autophagy in MCF-7 and MDA-MB-231 cells. miR-200b and miR-217 negatively regulated the expression of autophagy marker proteins. Chromatin immunoprecipitation assays showed the direct regulation of ATG-5. The decreased expression of ATG-5 by siRNA increased the sensitivity to anti-cancer drugs in MDA-MB-231 cells. In conclusion, DDX53 promotes stem cell-like properties, autophagy, and confers resistance to anti-cancer drugs in breast cancer cells.

Keywords: anti-cancer drug-resistance, autophagy, DDX53, EGFR, stem cell-like properties

INTRODUCTION

The expression of DDX53, cancer/testis antigen, is restricted to the testis (Cho et al., 2002). DDX53 is present in the sera of various cancers (Cho et al., 2002; Iwata et al., 2005; Liggins et al., 2010). DDX53 functions as an oncogene and increases the level of cyclins (Por et al., 2010). DDX53 confers resistance to anti-cancer drugs via negative regulation of p53 (Kim et al., 2010). miR-200b (Kim et al., 2013) and miR-217 (Kim et al., 2016) negatively regulate DDX53 and confer sensitivity to anti-cancer drugs.

Side population (SP) cells contain cancer-initiating cells with stemness characteristics. SP cells show higher expression of MDR1, NANOG, SOX-2, CD44 and CD133 (Xiong et al., 2014). SP cells possess abnormal cell cycle, high drug effluxes and high autophagic fluxes (Du et al., 2015). Cancer/testis antigens are overexpressed in cancer stem-like cells and in various cancers (Yang et al., 2015). MAGEA-3, cancer/testis antigen, is expressed in SP and main population (MP) cells derived from human bladder cancer SW780 cells (Yin et al., 2014).

MicroRNAs (miRNAs) or non-coding RNAs are key regulators of SP and cancer stem cells in general, leading to the initiation, development and progression of many malignancies. The micro RNA-200b (miR-200b) reduces erlotinib resistance of lung cancer cells and cancer stem cell markers (Ahmad et al., 2013). miR-29b inhibits cancer stemness (Chung et al., 2015). The decreased expression of miR-451

Received 26 October, 2016; revised 14 December, 2016; accepted 19 December, 2016; published online 26 January, 2017

eISSN: 0219-1032

decreases the expression of MDR1 and reduces the clonogenicity of SP cells (Du et al, 2015). miR-1181 inhibits the CSC (cancer stem cell)-like phenotypes in pancreatic cancer (Jiang et al., 2015). The decreased expression of miRNA-148a by DNMT1, suppresses glioblastoma cell stem-like properties and tumorigenic potential (Lopez-Bertoni et al., 2015). miR-200c decreases the expression of Sox2 to inhibit the phosphoinositide 3-kinase (PI3K)-AKT pathway (Lu et al., 2014). The decreased expression of miR-638 promotes invasion and a mesenchymal-like transition by exerting regulation on SOX2 *in vitro* (Ma et al., 2014). By modulating Oct4/Sox2 expression, the Lin28B-Let7 pathway regulates stemness properties in oral squamous cell carcinoma cells (Chien et al., 2015).

The inhibition of autophagy increases sensitivity to gemcitabine, mitomycin and cisplatin (Ojha et al., 2014). Inhibition of JAK2-mediated autophagy decreases the proportion of side population, tumor sphere forming ability and expression of stemness genes (Ojha et al., 2016). Inhibition Atg-5-mediated autophagy prevents cisplatin resistance by galectin-1 in hepatic cancer cells (Su et al., 2016). Knockdown of LC3, a marker of autophagy, leads to reduction of pluripotency in hESCs (Cho et al., 2014). BRAF increases the level of autophagic markers, such as LC3 and BECN1, in colorectal cancer cells (Goulielmaki et al., 2016). miR-21 mimics in hepatic cancer cells restore sorafenib resistance by inhibiting autophagy (He et al., 2015).

In this study, we showed a close relationship between autophagy and anti-cancer drug-resistance in breast cancer cells. We showed novel roles of DDX53 in autophagy and in promoting cancer stem-cell like properties.

MATERIALS AND METHODS

Cell culture

Cells were grown in DMEM containing heat-inactivated fetal bovine serum. Cultures were maintained in 5% CO_2 at 37℃.

Materials

Chemicals in this study were purchased from Sigma Company. Transfection reagents were purchased from Invitrogen (USA). All oligonucleotides used in this study were purchased from Bioneer Co. (Korea).

Flow cytometry

For CD133 surface expression analyses, viable cells (10^6 cells/ml) were incubated at 4℃ for 30 min with anti-CD133/1-PE (Miltenyi Biotec, Germany) following treatment with FcR Blocking Reagent (Miltenyi Biotec, Germany) and washed twice with PBS. Flow cytometry was carried out using a FACSCalibur (BD Biosciences, USA). Isotype-matched mouse IgG2b-PE antibodies served as controls.

Isolation of $CD133^+$ and $CD133^-$ Cells

$CD133^+$ and $CD133^-$ Cells were isolated from breast cancer cells by magnetic bead sorting using the MACs system (Miltenyi Biotec, Germany). For separation, cells were incubated with CD133 MicroBeads (100 μl/10^8 cells) for 30 min at 4℃ following treatment with FcR Blocking Reagent. Cells were selected by MS columns (Miltenyi Biotec, Germany), which retained $CD133^+$ cells linked by beads. Purity of isolated cells was evaluated by Western blotting. The fresh isolated $CD133^+$ cells were cultured before assay in a stem cell medium containing serum-free DMEM/F12 medium (Gibco-BRL, USA), 20 ng/ml epidermal growth factor (EGF) (Sigma), 10 ng/ml basic fibroblast growth factor (bFGF) (Sigma), and 20 ng/ml leukemia inhibitor factor (LIF) (Sigma).

Tumor sphere-forming potential assay

For tumorsphere forming assay, cells were seeded in 6-well plates (Corning Inc., USA) in the form of single cell suspensions (10^4 cells/well) and added with serum-free stem cell medium. All plates were maintained at 37℃ in a humidified incubator. During incubation, the cells were fed with 0.1 ml of serum-free stem cell medium on days 2, 4 and 6. Tumorspheres were observed by inverted microscopy (Olympus, Japan). The total number of tumorspheres was counted after 5-14 days of culture.

Western blot analysis

Western blot analysis and immunoprecipitation were carried out according to the standard procedures (Kim et al., 2014).

Chromatin immunoprecipitation (ChIP) Assays

For detection of binding of DDX53 protein to EGFR promoter sequences, EGFR promoter-1 sequences [5′-CCACGGCTG TTTGTGTCAAG-3′ (sense) and 5′-CCTTTATTCGGGTCCCCACC -3′ (antisense)], EGFR promoter-2 sequences [5′-ACAGATTT GGCTCGACCTGG-3′ (sense) and 5′-AGGAGGAGGGAGGA GAACCA-3′ (antisense)] and EGFR promoter-3 sequences [5′-AGCTAGACGTCCGGGCA-3′ (sense) and 5′-CCGGCTCTC CCGATCAATAC-3′ (antisense)] were used. Specific primers of ATG-5 promoter-1 sequences [5′-TTTAGAATGGGGAATG GGTTT-3′ (sense) and 5′-AGAGGAGCTTCACCTATACC-3′ (antisense)], ATG-5 promoter-2 sequences [5′-CTTCTGGGC TTGAAAGACTG-3′ (sense) and 5′-AATCCATGCCATAAAGAT TATCC-3′ (antisense)] were also used.

Cell viability determination

Cellular growth activity and viable cell counting were determined by MTT assays and trypan blue exclusion assays, respectively.

Capsase-3 activity assays

Caspase-3 activity was measured according to the standard procedures (Kim et al., 2013).

Transfection

Lipofectamine and Plus reagents (Invitrogen) were used for transfection.

Invasion and wound migration assays

Chemo invasion and wound migration assays were carried as described elsewhere (Kim et al., 2013).

Immunofluorescence staining

Cells were fixed in paraformaldehyde (4%) at 4℃ for 10 min and permeabilized with 0.01% Triton X-100. After blocking

with 10% BSA for 1 h, cells were stained with rabbit anti-human LC3 antibody (Cell Signaling Technology, BA) overnight at 4℃. After washing, cells were incubated with secondary anti-rabbit IgG Alexa 488 for 1 h in the dark. Unbound antibody was removed with PBS, cells were analyzed using a confocal microscopy. To study the co-localization of LC3 and p62, rabbit anti-LC3 and rabbit anti-p62 (Santa Cruz, 1:100) antibodies were used. First, cells were stained with rabbit anti-LC3 antibody and secondary anti-rabbit IgG Alexa-488. Cells were then stained with rabbit anti-p62 antibody following treatment with 10% BSA for 1 h. After washing with PBS, anti-rabbit IgG Alexa-568 secondary antibody was added for 1 h and analyzed using a confocal microscopy.

Statistical analysis

Statistical differences were determined by Student's *t* test.

RESULTS

DDX53 shows co-expression pattern with CD133, a marker of cancer stemness, in breast cancer cells

MDA-MB-231cells, a highly malignant triple-negative breast cancer cells, showed increased expression of CD133 compared to MCF-7 and SK-BR3 cells in flow cytometry analysis (Fig. 1A). MDA-MB-231cells showed increased expression of DDX53, EGFR and SOX-2 compared to MCF-7 and SK-BR3 cells (Fig. 1B). MDA-MB-231-CD133 ($^{+}$) cells showed higher level of DDX53, SOX-2, NANOG and MDR1 than MDA-MB-231-CD133 (-) cells (Fig. 1B). SOX-2 expression promotes proliferation of a subset of EGFR mutant lung cancer cells (Dogan et al, 2014). SOX-2 is necessary for cancer stemness (Liu et al., 2013). SOX-2 is closely related with epithelial-mesenchymal transitions (Luo et al., 2013). DDX53 increased tumor spheroid formation (self-renewal activity) in MCF-7 cells while the down-regulation of DDX53 by siRNA decreased tumor spheroid formation in MDA-MB-231 cells (Fig. 1C). DDX53 regulated the level of SOX-2 in (Fig. 1C). Therefore, DDX53 might regulate cancer stem cell-like properties.

DDX53 promotes cancer stem cell-like properties

The decreased expression of DDX53 by siRNA in MDA-MB-231-CD133 ($^{+}$) cells decreased the level of SOX-2, NANOG and MDR1 (Fig. 2A) and decreased tumor spheroid formation (Fig. 2B). Celastrol or cisplatin did not affect tumor spheroid forming potential of MDA-MB-231-CD133 ($^{+}$) cells (Fig. 2B). DDX53 increased the level of SOX-2, NANOG and MDR1 in (Fig. 2C) and tumor spheroid formation in MDA-MB-231-CD133 ($^{-}$) cells (Fig. 2D). Therefore, DDX53 may regulate stem cell-like properties.

DDX53 interacts with EGFR

DDX53-miR-217 feedback loop regulates the expression of EGFR in melanoma cells (Kim et al., 2016). The possibility of an interaction between DDX53 and EGFR was examined. The decreased expression of DDX53 by siRNA decreased the expression of EGFR in MDA-MB-231 while increasing the expression of EGFR in MCF-7 cells (Fig. 3A). DDX53 showed binding to EGFR in MDA-MB-231 cells (Fig. 3B). miR-200b inhibitor (Fig. 3C) and miR-217 inhibitor (Fig. 3D) increased the level of DDX53 and induced the binding of DDX53 to EGFR in MCF-7 cells. DDX53, by interacting with EGFR, may promote stem cell-like properties.

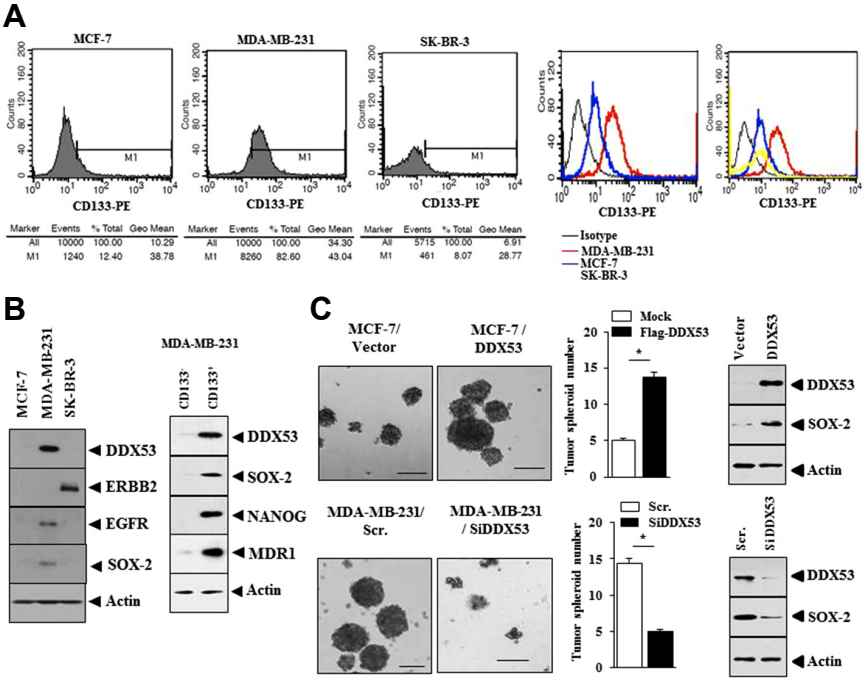

Fig. 1. DDX53 shows co-expression pattern with CD133. (A) Shows flow cytometry analysis to determine the expression of CD133. (B) Cell lysates were subjected to Western blot analysis. (C) Cancer cells were transfected with the indicated siRNA (10 nM), control vector (1 μg) or DDX53 (1 μg). At 48 h after transfection, tumor spheroid formation assays (left panel) and Western blot analysis were carried out (right panel). *$p < 0.05$.

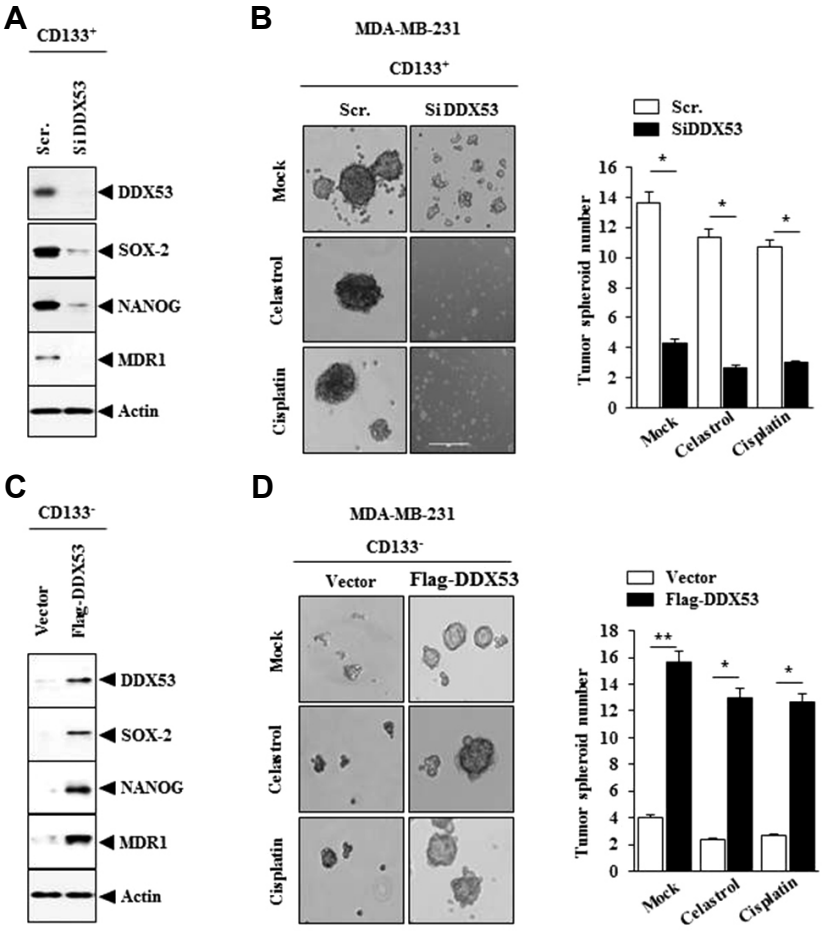

Fig. 2. DDX53 regulates cancer stem cell-like properties of MDA-MB-231 cells. (A) MDA-MB-231 cells were transfected with the indicated siRNA (10 nM). At 48 h after transfection, Western blot analysis was carried out. (B) MDA-MB-231 ($CD133^+$) cells were transfected with the indicated siRNA (10 nM) in the absence or presence of celastrol (2 μM) or cisplatin (150 μM), followed by tumor spheroid formation assays. * $p < 0.05$. (C) MDA-MB-231 ($CD133^-$) cells were transfected with the indicated construct (1 μg). Western blot analysis was carried out. (D) MDA-MB-231 ($CD133^-$) cells were transfected with the indicated construct (1 μg) in the absence or presence of celatsrol (2 μM) or cisplatin (150 μM), followed by tumor spheroid formation assays. *$p < 0.05$; **$p < 0.005$.

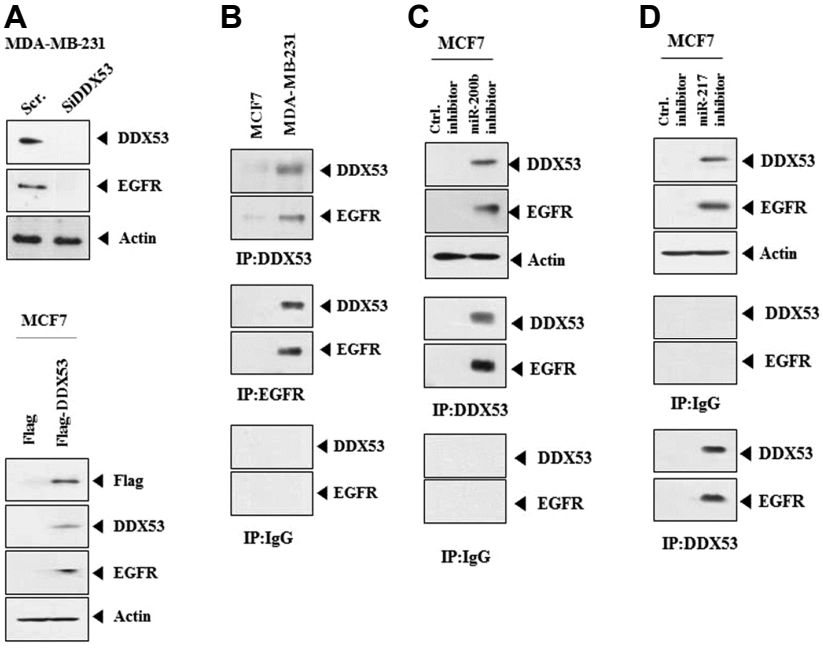

Fig. 3. DDX53 interacts with EGFR. (A) MDA-MB-231 cells were transfected with the indicated siRNA (10 nM). Western blot analysis was carried out (upper panel). MCF-7 cells were transfected with the indicated construct (1 μg). Western blot analysis was carried out (lower panel). (B) Cell lysates were immunoprecipitated with the indicated antibody (2 μg /ml), followed by Western blot analysis.

DDX53 directly increases the expression of EGFR

ChIP assays showed the binding of DDX53 to the promoter sequences of EGFR (Fig. 4A). The miR-200b inhibitor and miR-217 inhibitor induced the binding of DDX53 to the promoter sequences of EGFR (Fig. 4B). Therefore, DDX53 may directly increase the expression of EGFR.

DDX53 confers anti-cancer drug-resistance

Next, we examined the effect of DDX53 on anti-cancer drug-resistance. The decreased expression of DDX53 by siRNA led to cleavage of PARP (Fig. 5A) and increased caspase-3 activity in response to anti-cancer drugs in MDA-MB-231 cells (Fig. 5B). DDX53 exerted negative effects on cleavage of PARP (Fig. 5C) and on increased capsase-3 activity by anti-cancer drugs in MCF-7 cells (Fig. 5D). DDX53 increased the invasion and migration of MCF-7 cells while the decreased expression of DDX53 by siRNA decreased the invasion and migration of MDA-MB-231 cells (Fig. 5E). The effect of DDX53 on stem cell-like properties maybe related with its effect on anti-cancer drug-resistance.

miR-200b and miR-217 enhance sensitivity to anti-cancer drugs

miR-200b or miR-217 induced the cleavage of PARP by various anti-cancer drugs in MDA-MB-231 (Fig. 6A). The down-regulation of miR-200b or miR-217 prevented the cleavage of PARP by various anti-cancer drugs in MCF-7 (Fig. 6B).

EGFR confers resistance to anti-cancer drugs

The decreased expression of EGFR by siRNA increased sensitivity to various anti-cancer drugs (Fig. 7A) and caspase-3 activity in response to anti-cancer drug in MDA-MB-231 cells (Fig. 7B). The decreased expression of EGFR by siRNA induced the cleavage of PARP in response to anti-cancer drug in MDA-MB-231 cells (Fig. 7C). The decreased expression of EGFR by siRNA decreased the invasion and migration of MDA-MB-231 cells (Fig. 7D). Therefore, there is a close relationship between anti-cancer drug-resistance and invasion and migration.

The inhibition of autophagy decreases the level of DDX53 while increasing the sensitivity to anti-cancer drugs

Many reports indicate the existence of a relationship between anti-cancer drug-resistance and autophagy (Su et al., 2016). We, therefore, examined the involvement of DDX53 in autophagy. Chloroquine (CQ), an inhibitor of autophagy, decreases the expression of DDX53 and pBeclin1^{Ser15} (Fig. 8A) while increasing the sensitivity to various anti-cancer drugs in MDA-MB-231 cells (Fig. 8B). CQ increased caspase-3 activity in response to various anti-cancer drugs (Fig. 8C). Therefore, DDX53 is involved in in autophagy, and there is a close relationship between the response to anti-cancer drugs and autophagy.

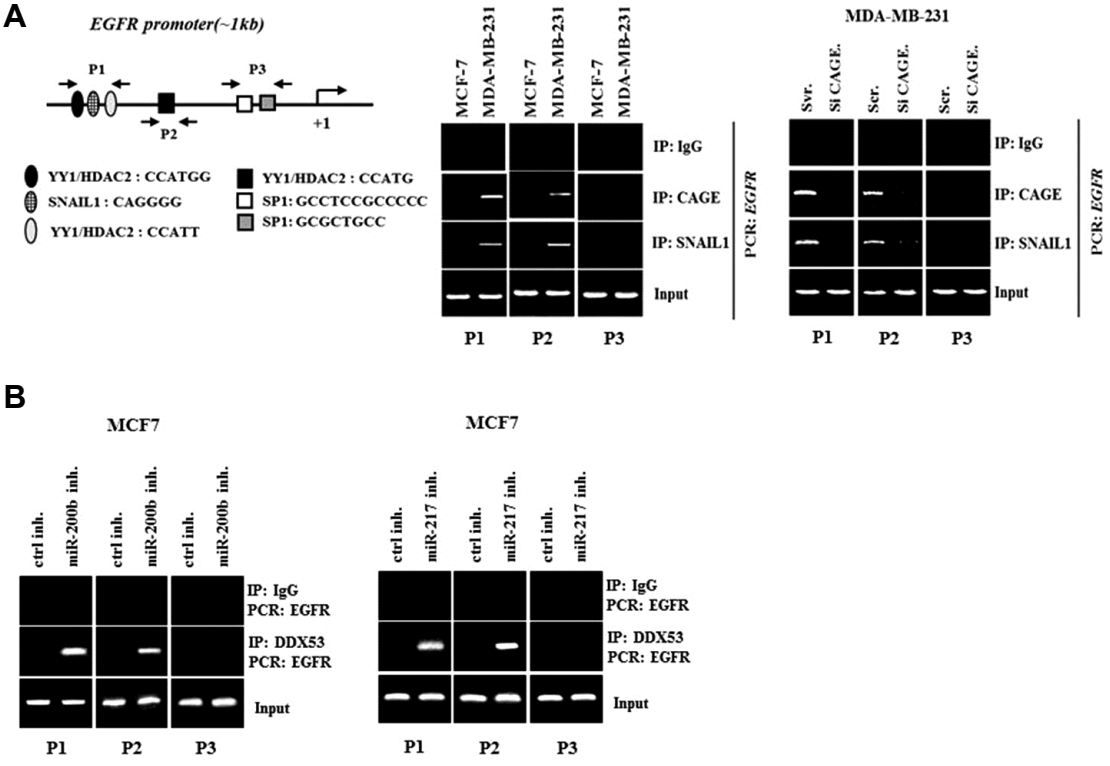

Fig. 4. DDX53 directly increases the expression of EGFR. (A) Shows potential binding sites for various transcription factors in the promoter sequences of EGFR (left panel). The cell lysates were subjected to ChIP assays employing the indicated antibody (2 μg/ml) (middle panel). MDA-MB-231 cells were transfected with the indicated siRNA (each at 10 nM). At 48 h after transfection, Western blot analysis was carried out (right panel). (B) MCF-7 cells were transfected with the indicated inhibitor (each at 10 nM), followed by ChIP assays.

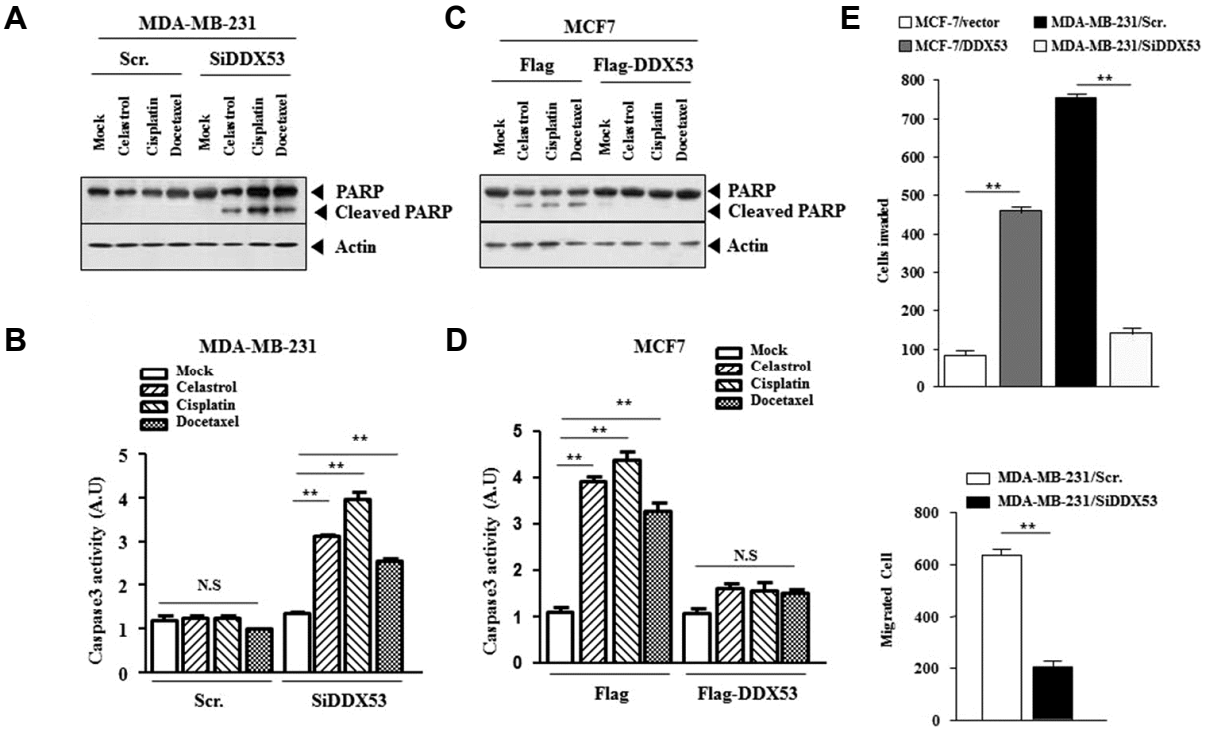

Fig. 5. DDX53 regulates the response to anti-cancer drugs. (A) MDA-MB-231 cells were transfected with the indicated siRNA (each at 10 nM). The next day, cells were the treated with the indicated anti-cancer drug (2 μM for celastrol; 150 μM for cisplatin; 50 nM for docetaxel) for 24 h, followed by Western blot analysis. (B) Same as A except that caspase-3 activity assays were carried out. **, < 0.005. (C) MCF-7 cells were transfected with the indicated construct (each at 1 μg), followed by Western blot analysis. (D) Caspase-3 activity assays were carried out. **p < 0.005. (E) MCF-7 cells were transfected with control vector (1 μg) or DDX53 (1 μg). MDA-MB-231 cells were transfected with the indicated siRNA (each at 10 nM). Invasion assays were carried out (upper panel). MDA-MB-231 cells were transfected with the indicated siRNA (each at 10 nM). Wound migration assays were carried out (lower panel). **p < 0.005.

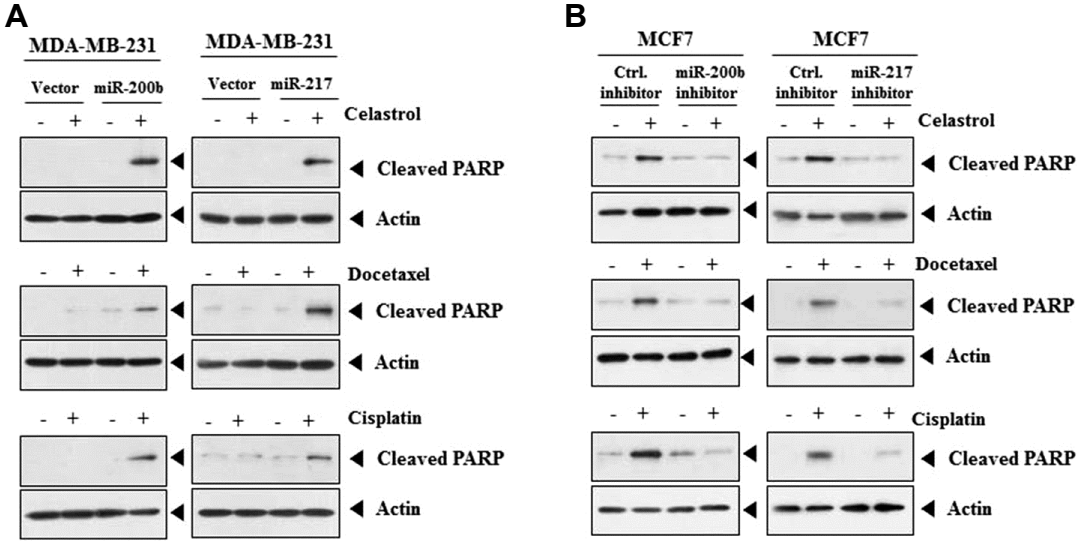

Fig. 6. miR-200b and miR-217 regulate the response to anti-cancer drugs. (A) MDA-MB-231 cells were transfected with control vector (1 μg), miR-200b (1 μg) or miR-217 (1 μg). The next day, cells were treated with the indicated anti-cancer drug (2 μM for celastrol; 150 μM for cisplatin; 50 nM for docetaxel) for 24 h, followed by Western blot analysis. (B) MCF-7 cells were transfected with the indicated inhibitor (each at 10 nM), followed by Western blot analysis.

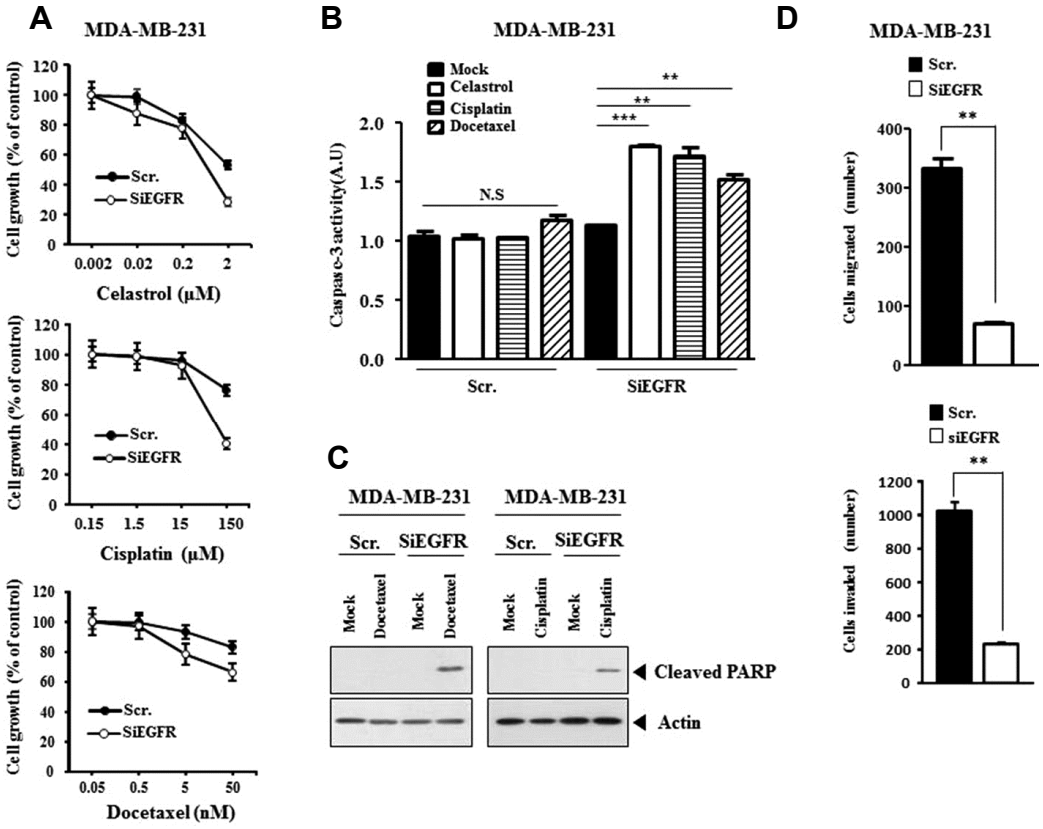

Fig. 7. EGFR regulates the response to anti-cancer drugs. (A) MDA-MB-231 cells were transfected with the indicated siRNA (each at 10 nM). The next day, cells were then treated with the indicated anti-cancer drug at various concentrations for 24 h, followed by MTT assays. (B) MDA-MB-231 cells were transfected with the indicated siRNA (each at 10 nM). The next day, cells were treated with the indicated anti-cancer drug (2 μM for celastrol; 150 μM for cisplatin; 50 nM for docetaxel) for 24 h, followed by caspase-3 activity assays **p < 0.005; ***p < 0.0005. (C) MDA-MB-231 cells were transfected with the indicated siRNA (each at 10 nM). The next day, cells were treated with the indicated anti-cancer drug (15 μM for cisplatin; 50 nM for docetaxel) for 24 h, followed by Western blot analysis. (D) MDA-MB-231 cells were transfected with the indicated siRNA (each at 10 nM). Migration (upper panel) or invasion (lower panel) assay was carried out. **p < 0.005.

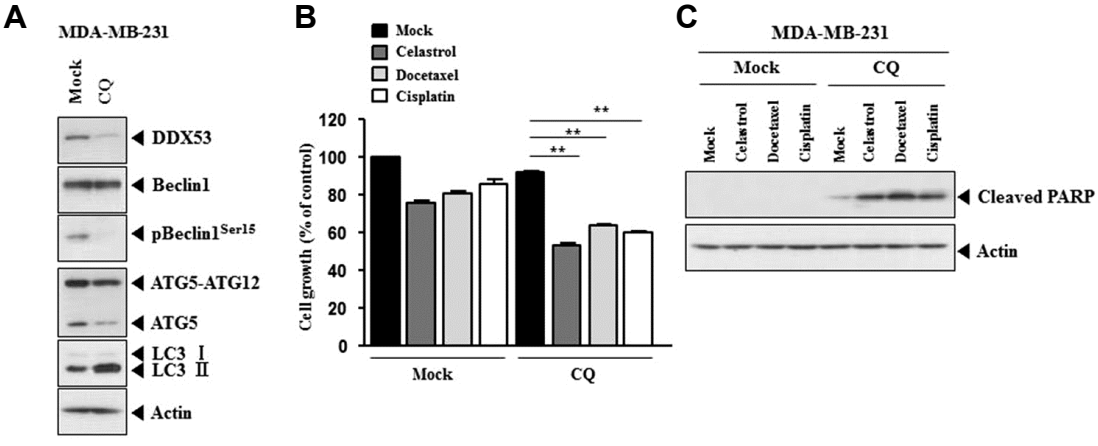

Fig. 8. The inhibition of autophagy decreases the expression of DDX53 and enhances the sensitivity to anti-cancer drugs. (A) MDA-MB-231 cells were treated with CQ (50 μM) for 24 h, followed by Western blot analysis. (B) MDA-MB-231 cells were treated with CQ (50 μM) for 24 h. After removal of CQ, cells were then treated with or without the indicated anti-cancer drug for 24 h. MDA-MB-231 cells untreated with CQ were also treated with the indicated anti-cancer drug for 24 h. MTT assays were carried out. **p < 0.005. (C) Same as B except that Western blot analysis was carried out.

DDX53 promotes autophagy

MDA-MB-231 cells showed higher expression of ATG-5-ATG12, LC-3I/II and pBeclin1^{Ser15} than MCF-7 cells (Fig. 9A). The decreased expression of DDX53 by siRNA decreased the level of ATG-5-ATG12, LC-3I/II and pBeclin1^{Ser15} in MDA-MB-231 cells (Fig. 9B). Full-length DDX53, but not DDX53 deletion construct, increased the level of ATG-5-ATG12, LC-3I/II and pBeclin1^{Ser15} in MCF-7 cells (Fig. 9C). MDA-MB-231 cells showed highly punctate pattern of LC-3I/II (Fig. 9D). The decreased expression of DDX53 by siRNA decreased the punctate pattern of LC-3I/II in MDA-MB-231 cells (Fig. 9D). Therefore, DDX53 promotes autophagy in breast cancer cells.

miR-200b and miR-217 regulate autophagy in breast cancer cells

The selective autophagic receptor p62, which associates directly with both ubiquitin and LC3, transports ubiquitin conjugates to autophagosomes for degradation (Park et al., 2016). The miR-200b inhibitor and miR-217 inhibitor increased the level of p62 along with DDX53, pBeclin1^{Ser15}, ATG-5 and LC3-I/II in MCF-7 cells (Fig. 10A). miR-200b and miR-217decreased the level of EGFR along with DDX53, pBeclin1^{Ser15}, ATG-5 and LC3-I/II in MDA-MB-231 (Fig. 10A). miR-200b inhibitor and miR-217 inhibitor increased punctate expression of LC-3I/II and p62 in MCF-7 cells (Fig. 10B). miR-200b inhibitor and miR-217 inhibitor induced co-localization of LC-3I/II with p62 in MCF-7 cells (Fig. 10B). MDA-MB-231 cells showed co-localization of LC-3I/II with p62 (Fig. 10B). miR-200b and miR-217 prevented co-localization of LC-3I/II with p62 in MDA-MB-231 cells (Fig. 10B). miR-200b and miR-217 decreased punctate expression of LC-3I/II and p62 in mDA-MB-231 cells (Fig. 10B). Therefore DDX53 promotes autophagy by increasing the punctate expression of p62 and inducing co-localization of p62 with LC-3.

DDX53 directly increases the expression of ATG-5

ATG-5 promoter contains binding sites for various transcription factors (Fig. 11A). DDX53 showed the binding to the promoter sequences of ATG-5 in MDA-MB-231 cells (Fig. 11B). miR-200b inhibitor and miR-217 inhibitor induced the binding of DDX53 to the promoter sequences of ATG-5 in MCF-7 cells (Fig. 11B). miR-200b or miR-217 prevented the biding of DDX53 to the promoter sequences of ATG-5 in MDA-MB-231 cells (Fig. 11C). Therefore DDX53 directly increases the expression of ATG-5.

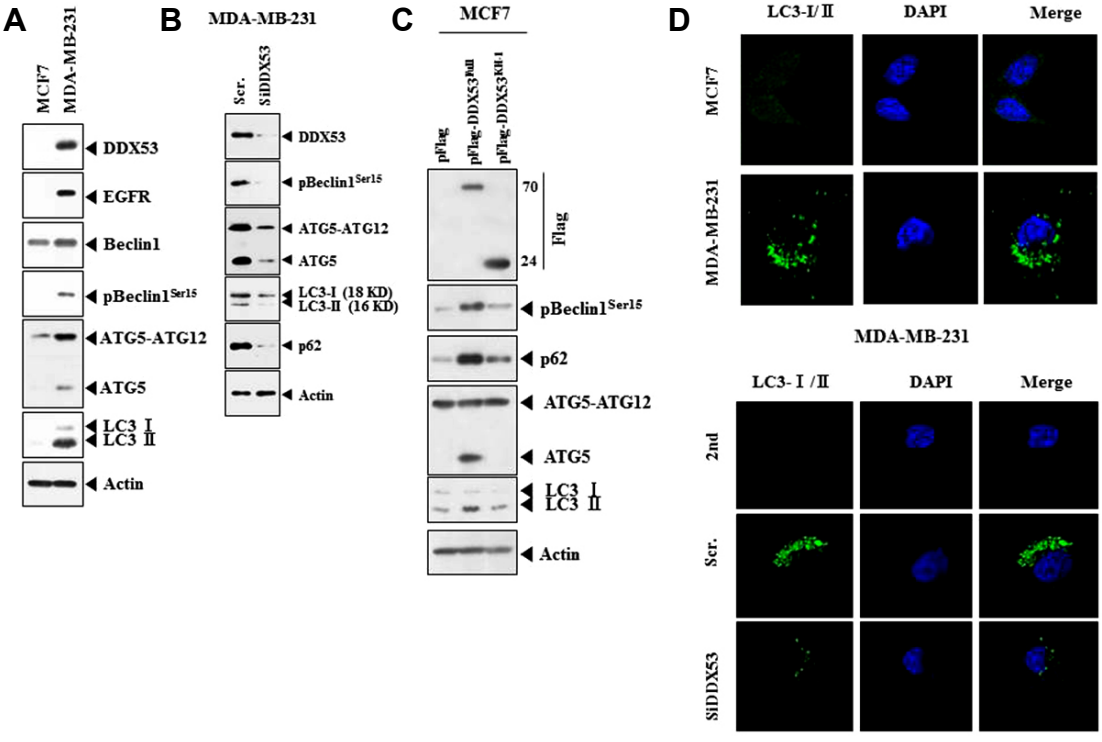

Fig. 9. DDX53 regulates autophagy. (A) Cell lysates isolated from the indicated cancer cells were subjected to Western blot analysis. (B) MDA-MB-231 cells were transfected with the indicated siRNA (each at 10 nM). Western blot analysis was performed. (C) MCF-7 cells were transfected with the indicated construct (each at 1 μg), followed by Western blot analysis. (D) Immunofluorescence staining employing LC-3I/II was performed (upper panel). MDA-MB-231 cells were transfected with the indicated siRNA (each at 10 nM), followed by immunofluorescence staining (lower panel).

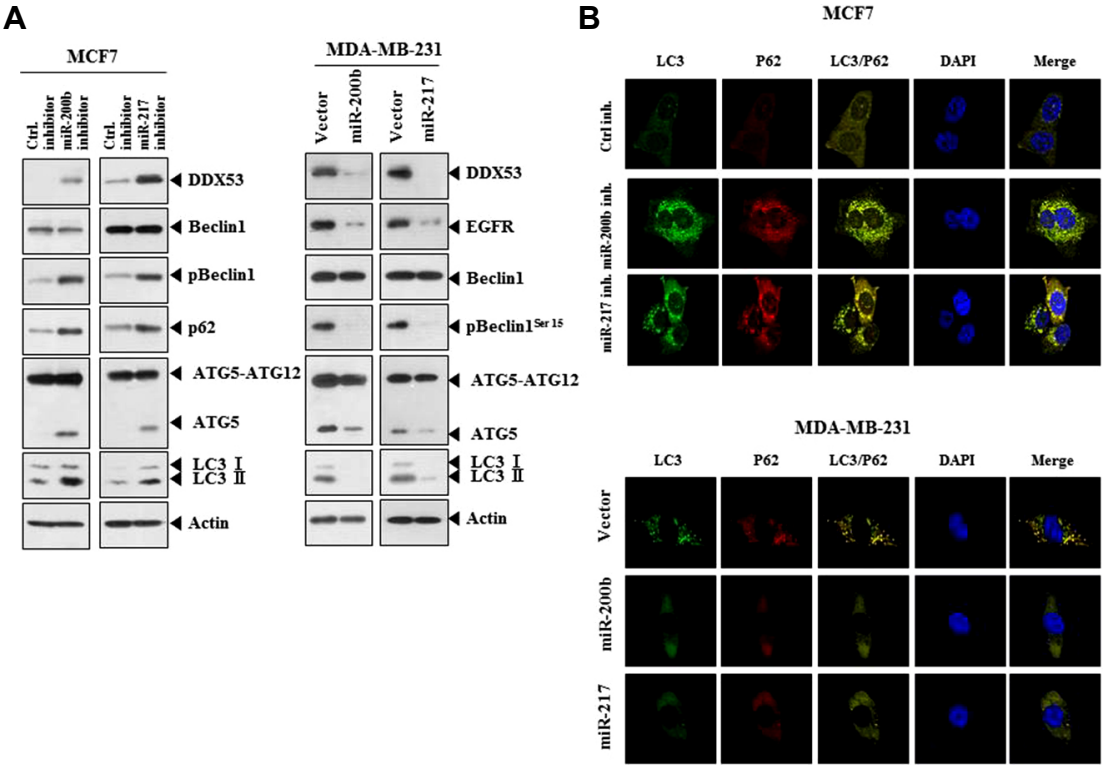

Fig. 10. miR-200b and miR-217 regulate autophagy. (A) MCF-7 cells were transfected with the indicated inhibitor (each at 10 nM), followed by Western blot analysis (left panel). MDA-MB-231 cells were transfected with the indicated construct (each at 1μg), followed by Western blot analysis (right panel). (B) Same as A except that immunofluorescence staining was carried out.

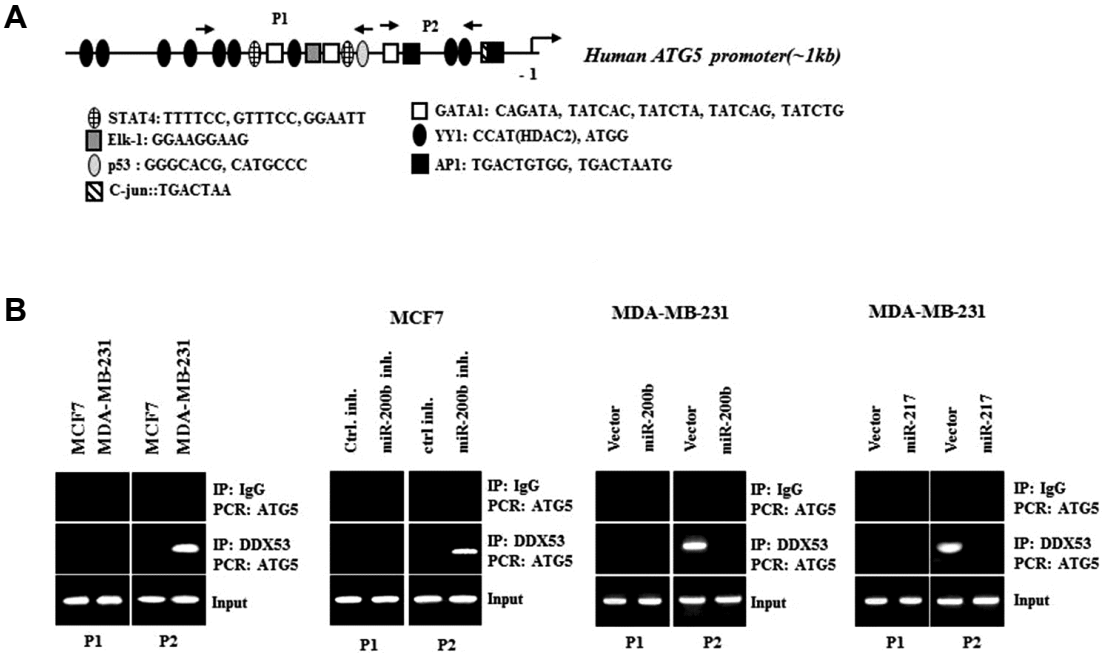

Fig. 11. DDX53 directly increases the expression of ATG-5. (A) Shows potential binding sites for various transcription factors in the promoter sequences of ATG-5. (B) Cells were subjected to ChIP assays (left panel). MCF-7 cells were transfected with the indicated inhibitor (each at 10 nM), followed by ChIP assays (right panel). (C) MDA-MB-231 cells were transfected with the indicated construct (each at 1 μg), followed by ChIP assays.

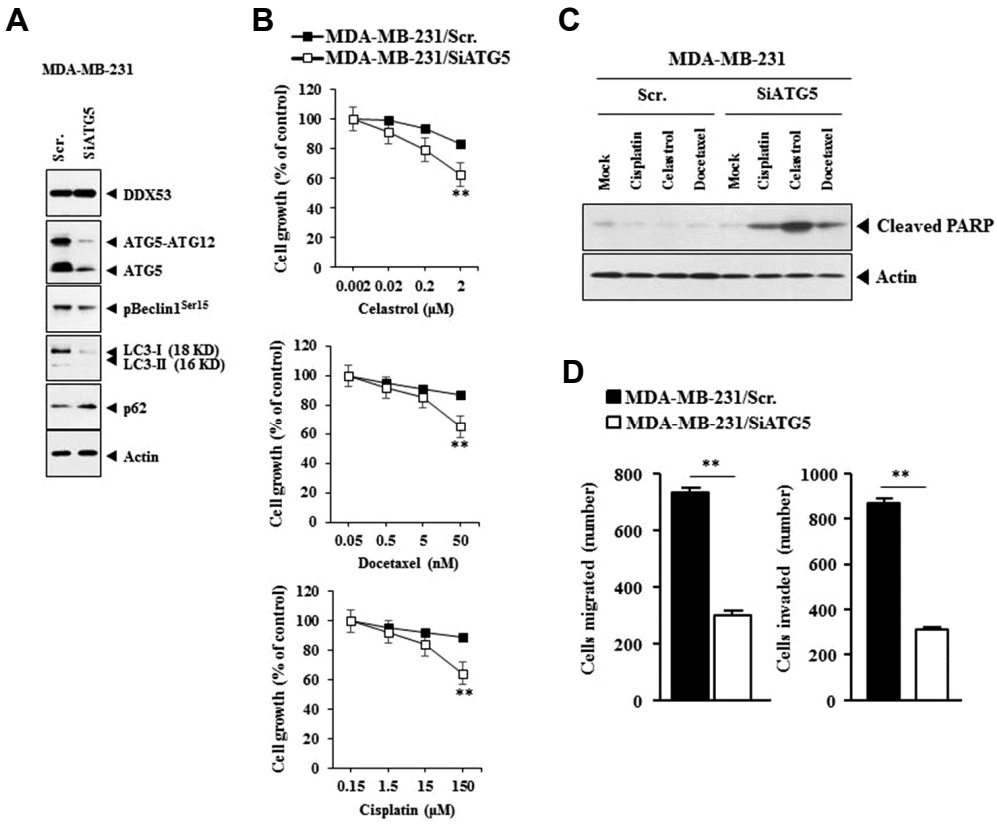

Fig. 12. The decreased expression of ATG-5 by siRNA confers sensitivity to anti-cancer drugs. (A) MDA-MB-231 cells were transfected with the indicated siRNA (each at 10 nM), followed by Western blot analysis. (B) MDA-MB-231 cells were transfected with the indicated siRNA (each at 10 nM). The next day, cells were then treated with the indicated anti-cancer drug at various concentrations for 24 h, followed by MTT assays. $^{**}p < 0.005$. (C) MDA-MB-231 cells were transfected with the indicated siRNA (each at 10 nM). The next day, cells were then treated with the indicated anti-cancer drug (2 μM for celastrol; 150 μM for cisplatin; 50 nM for docetaxel) for 24 h, followed by Western blot analysis. (D) MDA-MB-231 cells were transfected with the indicated siRNA (each at 10 nM), followed by migration and invasion assays. $^{**}p < 0.005$.

The decreased expression of ATG-5 by siRNA confers sensitivity to anti-cancer drugs

The decreased expression of ATG-5 by siRNA decreased the level of ATG-5-ATG12 and LC-3I/II, but not the expression of DDX53 (Fig. 12A). This suggest that ATG-5 functions downstream of DDX53. The decreased expression of ATG-5 by siRNA increased the sensitivity to anti-cancer drugs (Fig. 12B) and led to cleavage of PARP in response to anti-cancer drugs in MDA-MB-231 cells (Fig. 12C). The decreased expression of ATG-5 by siRNA decreased the migration of MDA-MB-231 cells (Fig. 12D). Therefore the effect of ATG-5 on autophagy is related with its effect on the sensitivity to anti-cancer drugs.

DISCUSSION

Autophagy is necessary for maintenance of $CD133^{+}$ LCSCs (liver cancer stem cells) under the oxygen- and nutrient-deprived conditions HCC (Song et al., 2013). Targeting CD133 by CD133mAb leads to cell death in HepG2 cells via inhibition of autophagic activity (Chen et al., 2013). Co-expression of DDX53 with CD133 in MDA-MB-231 suggests potential role of DDX53 in cancer stemness. SOX-2 regulates cancer stem cell-like properties (Chien et al., 2015). Because DDX53 regulates the expression of SOX-2, it may be reasonable that SOX-2 is directly regulated by DDX53.

Inhibition of celastrol-induced autophagic degradation of prevents celastrol-mediated cell death in gefitinib-resistant NSCLCs (Xu et al., 2016). The inhibition of EGFR increases in autophagy resulting in increased cell death under hypoxia (Chen et al., 2016). EGFR regulates cancer stem cell-like properties in colorectal cancer cells (Valverde et al., 2015). The fact that DDX53 binds to EGFR in MDA-MB-231 cells indicate that DDX53 regulates cancer stem cell-like properties through EGFR.

Cancer stem cell-like properties are associated with the silencing of miR-200b (Tellez et al., 2011). miR-200b inhibits autophagy and enhances the chemosensitivity of SPC-A1/DTX and H1299/DTX cells both *in vivo* and *in vitro* by decreasing the expression of ATG12 (Pan et al., 2015). miR-200b decreases the expression of EGFR and increases sensitivity to anti-cancer drugs in lung cancer cells (Zhen et al., 2015). miR-217 inhibits EGFR activation in melanoma cells

(Kim et al., 2016). In this study, miR-200b inhibitor and miR-217 inhibitor increases the expression of EGFR in MCF-7 cells and induce an interaction between DDX53 and EGFR. Therefore, miR-200b and miR-217 may regulate autophagy and cancer stem-cell like properties. EGFR/Stat3/Sox-2 signaling pathway regulates cancer stemness in breast cancer cells (Yang et al., 2013). EGFR-SOX2 is critical for self-renewal of human prostate cancer stem-like cells (Rybak and Tang, 2013). It would be interesting to determine domain of DDX53 necessary for an interaction with EGFR. It would be interesting to examine whether DDX53 increases the phosphorylation of EGFR in breast cancer cells.

Autophagy confers resistance to anti-cancer drugs in hepatocellular carcinoma (Su et al., 2015). We show the regulation of autophagy by DDX53 in MCF-7 and MDA-MB-231 cells. These results indicate novel role of DDX53 in autophagy. The identification of domain of DDX53 necessary for autophagy is the subject of ongoing investigation. Atg-5 knockout eliminates bortezomib-induced autophagosome formation and reduces susceptibility to bortezomib (Jaganathan et al., 2014). Inhibition of autophagy by silencing ATG-5, ATG7, and BECN1 or the administration of CQ reduces the CSC populations, sphere formation, and resistance to gemcitabine (Yang et al., 2015). The inhibition of PDT-induced autophagy by silencing of the ATG-5 gene results in apoptosis of PROM1/CD133 ($^{+}$) cells and decreases colonosphere formation *in vitro* and tumorigenicity *in vivo* (Wei et al., 2014). These reports suggest the role of ATG-5 in autophagy, cancer stemness and anti-cancer drug-resistance. In this study, we show the effect of ATG-5 on the sensitivity to anti-cancer drugs.

We report novel role of DDX53 in autophagy and cancer stem cell-like properties. We present evidence that DDX53 serves as a target for the development of anti-cancer therapeutics for the treatment of breast cancer patients expressing DDX53. Further studies are needed to understand the mechanism of DDX53 and to identify DDX53-miRNA network.

ACKNOWLEDGMENTS

This work was supported by National Research Foundation Grants (2014R1A2A2A01002448, 2015R1A1A3A04001339, 2015R1A2A1A15051678 and 2016R1A6A3A01006416), a grant from the BK21 plus Program, and grants from Kangwon National University (120150086 and 520160302).

REFERENCES

Ahmad, A., Maitah, M.Y., Ginnebaugh, K.R., Li, Y., Bao, B., Gadgeel, S.M., and Sarkar, F.H. (2013). Inhibition of Hedgehog signaling sensitizes NSCLC cells to standard therapies through modulation of EMT-regulating miRNAs. J. Hematol. Oncol. *6,* 77.

Chen, H., Luo, Z., Dong, L., Tan, Y., Yang, J., Feng, G., Wu, M., Li, Z., and Wang, H. (2013). CD133/prominin-1-mediated autophagy and glucose uptake beneficial for hepatoma cell survival. PLoS One *8,* e56878.

Chen, Y., Henson, E.S., Xiao, W., Huang, D., McMillan-Ward, E.M., Israels, S.J., and Gibson, S.B. (2016). Tyrosine kinase receptor EGFR regulates the switch in cancer cells between cell survival and cell death induced by autophagy in hypoxia. Autophagy *12,* 1029-1046.

Chien, C.S., Wang, M.L., Chu, P.Y., Chang, Y.L., Liu, W.H., Yu, C.C., Lan, Y.T., Huang, P.I., Lee, Y.Y., Chen, Y.W., et al. (2015). Lin28B/Let-7 Regulates Expression of Oct4 and Sox2 and Reprograms Oral Squamous Cell Carcinoma Cells to a Stem-like State. Cancer Res. *75,* 2553-2565.

Cho, B., Lim, Y., Lee, D.Y., Park S,Y., Lee, H., Kim, W.H., Yang, H., Bang, Y.J., and Jeoung, D.I. (2002). Identification and characterization of a novel cancer/testis antigen gene CAGE. Biochem. Biophys. Res. Commun. *292,* 715-726.

Cho, Y.H., Han, K.M., Kim, D., Lee, J., Lee, S.H., Choi, K.W., Kim, J., and Han, Y.M. (2014). Autophagy regulates homeostasis of pluripotency-associated proteins in hESCs. Stem Cells *32,* 424-435.

Chung, H.J., Choi, Y.E., Kim, E.S., Han, Y.H., Park, M.J., and Bae, I.H. (2015). miR-29b attenuates tumorigenicity and stemness maintenance in human glioblastoma multiforme by directly targeting BCL2L2. Oncotarget *6,* 18429-18444.

Dogan, I., Kawabata, S., Bergbower, E., Gills, J.J., Ekmekci, A., Wilson, W., Rudin, C.M., and Dennis, P.A. (2014). SOX2 expression is an early event in a murine model of EGFR mutant lung cancer and promotes proliferation of a subset of EGFR mutant lung adenocarcinoma cell lines. Lung Cancer *85,* 1-6.

Du, J., Liu, S., He, J., Liu, X., Qu, Y., Yan, W., Fan, J., Li, R., Xi, H., Fu, W., et al. (2015). MicroRNA-451 regulates stemness of side population cells via PI3K/Akt/mTOR signaling pathway in multiple myeloma. Oncotarget *6,* 14993-15007.

Goulielmaki, M., Koustas, E., Moysidou, E., Vlassi, M., Sasazuki, T., Shirasawa, S., Zografos, G., Oikonomou, E., and Pintzas, A. (2016). BRAF associated autophagy exploitation: BRAF and autophagy inhibitors synergise to efficiently overcome resistance of BRAF mutant colorectal cancer cells. Oncotarget *7,* 9188-9221.

He, C., Dong, X., Zhai, B., Jiang, X., Dong, D., Li, B., Jiang, H., Xu, S., and Sun, X. (2015). MiR-21 mediates sorafenib resistance of hepatocellular carcinoma cells by inhibiting autophagy via the PTEN/Akt pathway. Oncotarget *6,* 28867-28881.

Iwata, T., Fujita, T., Hirao, N., Matsuzaki, Y., Okada, T, Mochimaru, H., Susumu, N., Matsumoto, E., Sugano, K., Yamashita, N., et al. (2005). Frequent immune responses to a cancer/testis antigen, CAGE, in patients with microsatellite instability-positive endometrial cancer. Clin. Cancer Res. *11,* 3949-3957.

Jaganathan, S., Malek, E., Vallabhapurapu, S., Vallabhapurapu, S., and Driscoll, J.J. (2014). Bortezomib induces AMPK-dependent autophagosome formation uncoupled from apoptosis in drug resistant cells. Oncotarget *5,* 12358-12370.

Jiang, J., Li, Z., Yu, C., Chen, M., Tian, S., and Sun, C. (2015). MiR-1181 inhibits stem cell-like phenotypes and suppresses SOX2 and STAT3 in human pancreatic cancer. Cancer Lett. *356,* 962-970.

Kim, Y., Park, H., Park, D., Lee, Y.S., Choe, J., Hahn, J.H., Lee, H., Kim, Y.M., and Jeoung, D. (2010). Cancer/testis antigen CAGE exerts negative regulation on p53 expression through HDAC2 and confers resistance to anti-cancer drugs. J. Biol. Chem. *285,* 25957-25968.

Kim, Y., Park, D., Kim, H., Choi, M., Lee, H., Lee, Y.S., Choe, J., Kim, Y.M., and Jeoung, D. (2013). miR-200b and cancer/testis antigen CAGE form a feedback loop to regulate the invasion and tumorigenic and angiogenic responses of a cancer cell line to microtubule-targeting drugs. J. Biol. Chem. *288,* 36502-36518.

Kim, Y., Kim, H., Park, H., Park, D., Lee, H., Lee, Y.S., Choe, J., Kim, Y.M., and Jeoung, D. (2014). miR-326-Histone Deacetylase-3 feedback loop regulates the invasion and tumorigenic and angiogenic response to anti-cancer drugs. J. Biol. Chem. *289,* 28019-28039.

Kim, Y., Kim, H., Park, D., Han, M., Lee, H., Lee, Y.S., Choe, J., Kim, Y.M., and Jeoung D. (2016). miR-217 and CAGE form feedback loop and regulates the response to anti-cancer drugs through EGFR and

HER2. Oncotarget *7,* 10297-10321.

Liggins, A.P., Lim, S.H., Soilleux, E.J., Pulford, K., and Banham, A.H. (2010). A panel of cancer-testis genes exhibiting broad-spectrum expression in haematological malignancies. Cancer Immun. *10,* 8.

Liu, K., Lin, B., Zhao, M., Yang, X., Chen, M., Gao, A., Liu, F., Que, J., and Lan, X. (2013). The multiple roles for Sox2 in stem cell maintenance and tumorigenesis. Cell Signal. *25,* 1264-1271.

Lopez-Bertoni, H., Lal, B., Li, A., Caplan, M., Guerrero-Cázares, H., Eberhart, C.G., Quiñones-Hinojosa, A., Glas, M., Scheffler, B., Laterra, J., et al. (2015). DNMT-dependent suppression of microRNA regulates the induction of GBM tumor-propagating phenotype by Oct4 and Sox2. Oncogene *34,* 3994-4004.

Lu, Y.X., Yuan, L., Xue, X.L., Zhou, M., Liu, Y., Zhang, C., Li, J.P., Zheng, L., Hong, M., and Li, X.N. (2014). Regulation of colorectal carcinoma stemness, growth, and metastasis by an miR-200c-Sox2-negative feedback loop mechanism. Clin. Cancer Res. *20,* 2631-2642.

Luo, W., Li, S., Peng, B., Ye, Y., Deng, X., and Yao, K. (2013). Embryonic stem cells markers SOX2, OCT4 and Nanog expression and their correlations with epithelial-mesenchymal transition in nasopharyngeal carcinoma. PLoS One *8,* e56324.

Ma, K., Pan, X., Fan, P., He, Y., Gu, J., Wang, W., Zhang, T., Li, Z., and Luo, X. (2014). Loss of miR-638 in vitro promotes cell invasion and a mesenchymal-like transition by influencing SOX2 expression in colorectal carcinoma cells. Mol. Cancer *13,* 118.

Ojha, R., Jha, V., Singh, S.K., and Bhattacharyya, S. (2014). Autophagy inhibition suppresses the tumorigenic potential of cancer stem cell enriched side population in bladder cancer. Biochim. Biophys. Acta. *1842,* 2073-2086.

Ojha, R., Singh, S.K., and Bhattacharyya, S. (2016). JAK-mediated autophagy regulates stemness and cell survival in cisplatin resistant bladder cancer cells. Biochim. Biophys. Acta *1860,* 2484-2497.

Ozen, M., Karatas, O.F., Gulluoglu, S., Bayrak, O.F., Sevli, S., Guzel, E., Ekici, I.D., Caskurlu, T., Solak, M., Creighton, C.J., et al. (2015). Overexpression of miR-145-5p inhibits proliferation of prostate cancer cells and reduces SOX2 expression. Cancer Invest. *33,* 251-258.

Pan, B., Feng, B., Chen, Y., Huang, G., Wang, R., Chen, L., and Song, H. (2015). MiR-200b regulates autophagy associated with chemoresistance in human lung adenocarcinoma. Oncotarget *6,* 32805-32820.

Park, S., Han, S., Choi, I., Kim, B., Park, S.P., Joe, E.H., and Suh, Y.H. (2016). Interplay between Leucine-Rich Repeat Kinase 2 (LRRK2) and p62/SQSTM-1 in Selective Autophagy. PLoS One *11,* e0163029.

Por, E., Byun, H.J., Lee, E.J., Lim, J.H., Jung, S.Y., Park, I., Kim, Y.M., Jeoung, D.I., and Lee, H. (2010). The cancer/testis antigen CAGE with oncogenic potential stimulates cell proliferation by up-regulating cyclins D1 and E in an AP-1- and E2F-dependent manner. J. Biol. Chem. *285,* 14475-14485.

Rybak, A.P., and Tang, D. (2013). SOX2 plays a critical role in EGFR-mediated self-renewal of human prostate cancer stem-like cells. Cell Signal *25,* 2734-2742.

Shankar, S., Nall, D., Tang, S.N., Meeker, D., Passarini, J., Sharma, J., and Srivastava, R.K. (2011). Resveratrol inhibits pancreatic cancer stem cell characteristics in human and KrasG12D transgenic mice by inhibiting pluripotency maintaining factors and epithelial-mesenchymal transition. PLoS One *6,* e16530.

Song, Y.J., Zhang, S.S., Guo, X.L., Sun, K., Han, Z.P., Li, R., Zhao, Q.D., Deng, W.J., Xie, X.Q., Zhang, J.W., et al. (2013). Autophagy contributes to the survival of CD133+ liver cancer stem cells in the hypoxic and nutrient-deprived tumor microenvironment. Cancer Lett. *339,* 70-81.

Su, Y.C., Davuluri, G.V., Chen, C.H., Shiau, D.C., Chen, C.C., Chen, C.L., Lin, Y.S., and Chang, C.P. (2016). Galectin-1-Induced Autophagy Facilitates Cisplatin Resistance of Hepatocellular Carcinoma. PLoS One *11,* e0148408.

Tang, M.C., Wu, M.Y., Hwang, M.H., Chang, Y.T., Huang, H.J., Lin, A.M., and Yang, J.C. (2015). Chloroquine enhances gefitinib cytotoxicity in gefitinib-resistant nonsmall cell lung cancer cells. PLoS One *10,* e0119135.

Tellez, C.S., Juri, D.E., Do, K., Bernauer, A.M., Thomas, C.L., Damiani, L.A., Tessema, M., Leng, S., and Belinsky, S.A. (2011). EMT and stem cell-like properties associated with miR-205 and miR-200 epigenetic silencing are early manifestations during carcinogen-induced transformation of human lung epithelial cells. Cancer Res. *71,* 3087-3097.

Valverde, A., Peñarando, J., Cañas, A., López-Sánchez, L.M., Conde, F., Hernández, V., Peralbo, E., López-Pedrera, C., de la Haba-Rodríguez, J., Aranda, E., et al. (2015). Simultaneous inhibition of EGFR/VEGFR and cyclooxygenase-2 targets stemness-related pathways in colorectal cancer cells. PLoS One *10,* e0131363

Wei, M.F., Chen, M.W., Chen, K.C., Lou, P.J., Lin, S.Y., Hung, S.C., Hsiao, M., Yao, C.J., and Shieh, M.J. (2014). Autophagy promotes resistance to photodynamic therapy-induced apoptosis selectively in colorectal cancer stem-like cells. Autophagy *10,* 1179-1192.

Xiong, B., Ma, L., Hu, X., Zhang, C., and Cheng, Y. (2104). Characterization of side population cells isolated from the colon cancer cell line SW480. Int. J. Oncol. *45,* 1175-1183.

Xu, S.W., Law, B.Y., Mok, S.W., Leung, E.L., Fan, X.X., Coghi, P.S., Zeng, W., Leung, C.H., Ma, D.L., Liu, L., et al. (2016). Autophagic degradation of epidermal growth factor receptor in gefitinib-resistant lung cancer by celastrol. Int. J. Oncol. *49,* 1576-1588.

Yang, J., Liao, D., Chen, C., Liu, Y., Chuang, T.H., Xiang, R., Markowitz, D., Reisfeld, R.A., and Luo, Y. (2013). Tumor-associated macrophages regulate murine breast cancer stem cells through a novel paracrine EGFR/Stat3/Sox-2 signaling pathway. Stem Cells *31,* 248-258.

Yang, M.C., Wang, H.C., Hou, Y.C., Tung, H.L., Chiu, T.J., and Shan, Y.S. (2015) Blockade of autophagy reduces pancreatic cancer stem cell activity and potentiates the tumoricidal effect of gemcitabine. Mol. Cancer *14,* 179.

Yang, P., Huo, Z., Liao, H., and Zhou, Q. (2015) Cancer/testis antigens trigger epithelial-mesenchymal transition and genesis of cancer stem-like cells. Curr. Pharm. Des. *21,* 1292-1300.

Yin, B., Zeng, Y., Liu, G., Wang, X., Wang, P., and Song, Y. (2014) MAGE-A3 is highly expressed in a cancer stem cell-like side population of bladder cancer cells. Int. J. Clin. Exp. Pathol. *7,* 2934-2941.

Zhen, Q., Liu, J., Gao, L., Liu, J., Wang, R., Chu, W., Zhang, Y., Tan, G., Zhao, X., and Lv, B. (2015) MicroRNA-200a targets EGFR and c-Met to inhibit migration, invasion, and gefitinib resistance in non-small cell lung cancer. Cytogenet. Genome Res. *146,* 1-8.